Red-light-emitting electrochemical cell using a polypyridyl iridium(III) polymer†

José Lorenzo Rodríguez-Redondo,[a] Rubén D. Costa,[b] Enrique Ortí,[b] Angela Sastre-Santos,[a] Henk J. Bolink*[b] and Fernando Fernández-Lázaro*[a]

Received 22nd May 2009, Accepted 11th September 2009
First published as an Advance Article on the web 29th September 2009
DOI: 10.1039/b910105e

A deep-red phosphorescent ionic iridium(III) complex is prepared and incorporated into a polymer. Both the complex (**1**) and the polymer (**2**) were used as the single active material in solid-state light-emitting electrochemical cells (LECs). The devices built up using **1** and **2** emit in the deep-red region of the visible spectrum with CIE coordinates $x = 0.710$; $y = 0.283$ and $x = 0.691$; $y = 0.289$, respectively, making them one of the deepest-red emitting LECs reported. It is the first example of a polymeric LEC incorporating an ionic iridium complex, which exhibits increased stabilities compared with the device based on the small molecular weight complex.

Introduction

Solid-state light-emitting electrochemical cells (LECs) have attracted considerable interest in the past few years.[1,2] LECs are single-component electroluminescent devices basically consisting of a film of a charged luminescent material deposited between two electrodes.[1,3] In its simplest form, LECs are made up of a single active layer composed of an ionic transition-metal complex (iTMC).[2,4,5] The presence of mobile counterions facilitates the formation of ionic junctions that lower the barrier for electron and hole injection and makes LECs independent of the work function of the electrode material.[6,7] These characteristics make them suitable for low-cost lighting and signing applications.[8] The compounds most widely used in these single-component devices are cationic ruthenium(II) and iridium(III) complexes.[2] Recently, a breakthrough in the stability of LECs was reported by the use of Ir-iTMCs that form supramolecular cages *via* intramolecular π–π stacking.[9–11]

A wide range of emission colours, including white,[12] and efficiencies as high as 36 lm W^{-1} have been reached.[13,14] However, only few examples of deep-red emitting LECs are reported.[15–18] Deep-red emitting LECs are of interest as they can be used in low-cost sensing applications.[19,20] The deep-red emitting LECs make use of cationic ruthenium(II) complexes exhibiting low photoluminescence quantum efficiencies (PLQE) that hence result in low-efficiency devices. Ir-iTMCs have much higher PLQEs than Ru-iTMCs and hence they are more interesting to be used in LECs. Ir-iTMCs can be tuned to emit in the deep-red region *via* proper selection of the ligands. A route towards a deep-red emitting Ir-iTMC is described in this work.

The iTMCs used in LECs have, in general, molecular weights below 1000 g mol^{-1}. Their low molecular weights allow for a good solubility in a wide range of solvents but sometimes complicate the formation of amorphous thin films. In some cases, it is possible to obtain transparent films from these low molecular weight iTMCs using solution-based processes that on a macroscale appear to be amorphous glasses. On a microscopic scale, however, the presence of nanoscale crystalline domains was revealed by grazing incident X-ray analysis for a film of tris(2,2′-bipyridine)-ruthenium(II) hexafluorophosphate ($[Ru(bpy)_3][PF_6]_2$).[21]

When the film formation is not straightforward, small amounts of an inactive polymer or ionic liquid must be added to improve film quality. Works on polymeric organic light-emitting diodes (OLEDs) have shown that the stability of the devices based on blends of active molecules is lower than that when these active components are covalently linked to each other. In analogy, it can be then expected that the stability of LECs can be improved by attaching iTMCs covalently to polymer chains. In such polymer-based LECs (PLECs) the iTMCs potential tendency to aggregate is strongly hindered hence ensuring easy solution processing. This concept of polymeric iTMCs has been applied to LECs only in the case of a ruthenium complex containing polymer,[22] but as yet has not been adopted for Ir-iTMCs.

In this work, both a low molecular weight deep-red light-emitting Ir-iTMC and a polymer incorporating that Ir-iTMC are prepared. The performance of the LEC devices prepared using them as the main active components is described. Both the small molecular complex (**1**) and the polymer (**2**) are capable of transporting electronic charges, both holes and electrons, and emit light. They are specially designed to have a short band gap, thus emitting in the deep-red of the visible spectrum, by the introduction of electron-withdrawing groups in the bipyridine (bpy) ligand. These groups stabilize the LUMO of the complex which is primarily located on the bpy ligand. The stability of the LECs is in the range of what is typically observed (24 to 48 h). The LECs based on the polymer have a notably longer stability (reaching a half life of 37 h) than those using the small molecular iTMC.

[a]*División de Química Orgánica, Instituto de Bioingeniería, Universidad Miguel Hernández, Elche, 03202, Spain. E-mail: fdofdez@umh.es*
[b]*Instituto de Ciencia Molecular, Universidad de Valencia, PO Box 22085, ES-46071, Valencia, Spain. E-mail: henk.bolink@uv.es*

† Electronic supplementary information (ESI) available: Partial ^{1}H-NMR of compounds **2** and **7**, DQF-COSY of compound **7**, HSQC of compounds **1** and **7**. See DOI: 10.1039/b910105e

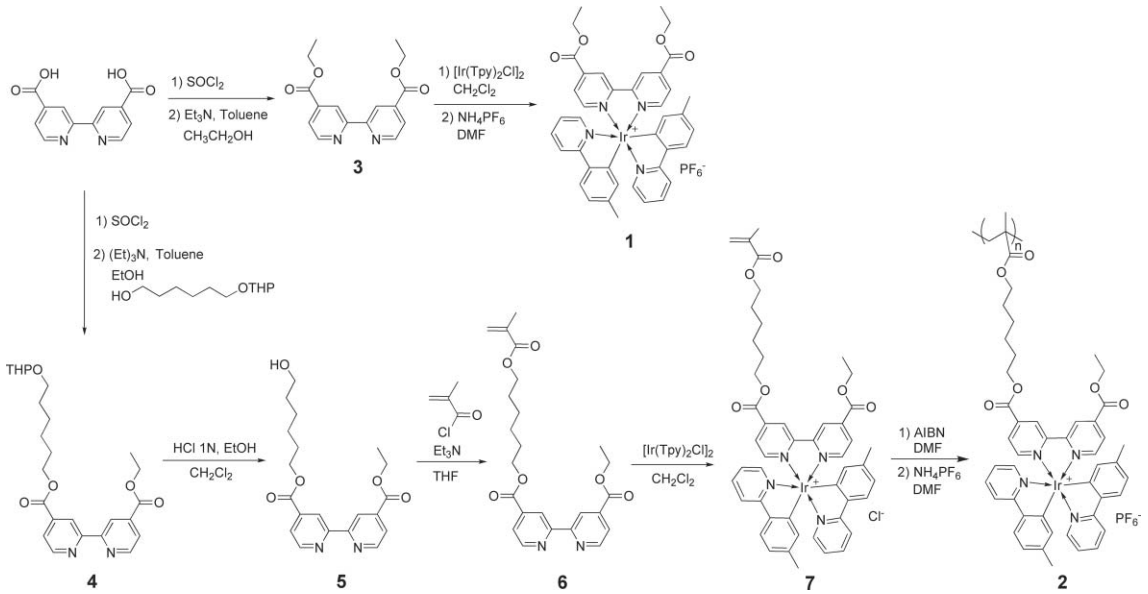

Scheme 1 Synthesis of iridium complex **1** and iridium polymer **2**.

Results and discussion

Synthesis

The synthetic procedures used to obtain both the ionic iridium(III) complex **1** and the related polymer **2** are displayed in Scheme 1. A hexyl chain is used to link the iridium complex to the polymer. This increases the solubility and reduces the interactions among Ir centres in the solid state, thus decreasing the excited-state self-quenching.[23,24]

The synthesis of the iridium complex **1** was achieved in *ca.* 50% yield by a standard procedure from the diester **3**[25,26] and the organometallated dimer $[Ir(Tpy)_2Cl]_2$ (where Tpy denotes tolylpiridine).

A statistical condensation was carried out to prepare the asymmetrically substituted bipyridine **4** in 42% yield, by reaction of the diacyl chloride derivative of the 2,2′-bipyridine-4,4′-dicarboxylic acid with a mixture of ethanol and 6-[(tetrahydro-2*H*-pyran-2′-yl)oxy]-1-hexanol. In this reaction, compound **3** (21%) and the di(THPO-hexyl) ester (13%) were also isolated as by-products. Deprotection of **4** in acidic medium to afford the alcohol **5**, followed by treatment with methacryloyl chloride yielded compound **6** in good yield. Reaction of the latter compound with the $[Ir(Tpy)_2Cl]_2$ dimer led to the monomeric mixed-macroligand iridium(III) complex **7** by a bridge-splitting reaction. Finally, the ionic homopolymer **2** was obtained as a red powder in 43% yield by a general synthetic procedure for the polymerization of methacrylates in the presence of AIBN, followed by precipitation with a saturated NH_4PF_6 solution using a counterion exchange process.

The formation of the polymer was easily demonstrated by comparing the ^{1}H-NMR spectra of the iridium monomer **7** and the iridium polymer **2**, because in the latter no signals attributable to olefinic protons, at 5.54 and 6.08 ppm, were found (see ESI).† The assignation of the protons of the iridium complexes were done by DQF-COSY and HSQC (see ESI).† Gel permeation chromatography (GPC) was used to measure the molecular weight of the polymer. Using NH_4PF_6-containing DMF as eluent with a flow rate of 1 mL min^{-1} at 70 °C (using polystyrene standards), $\tilde{M}_n$ and $\tilde{M}_w$ values of 38 000 and 53 000 Da and PDI of 1.4 were calculated. Thermal analysis using DSC was performed for polymer **2** showing a glass transition temperature of 174 °C.

Photophysical characterization

Fig. 1 displays the absorption and emission spectra recorded for the iridium complex **1** and the iridium polymer **2** at room temperature. The absorption spectrum of both **1** and **2** in acetonitrile shows an intense band in the UV zone at 270–300 nm, and a second less-intense band centred around 377 nm. The appearance of the absorption spectrum is typical of heteroleptic iridium complexes and shows that the complex is nearly colourless, with only a slight yellowish hue due to the absorption bordering the blue region of the visible spectrum. The high-energy absorption bands are attributed to ligand centred $\pi \rightarrow \pi^*$ transitions, whereas the broad

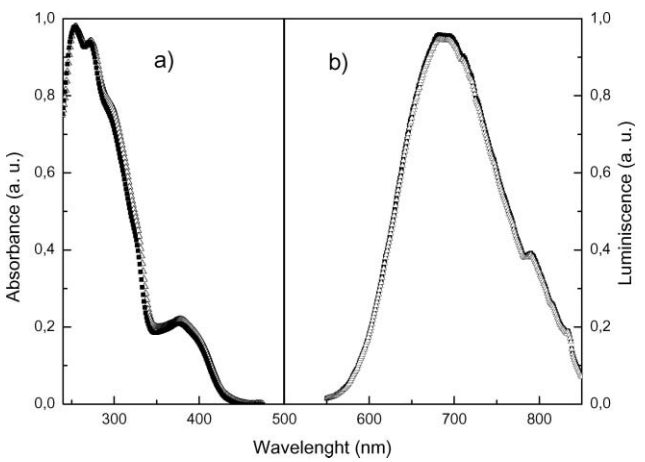

Fig. 1 (a) UV-vis spectra of complex **1** (open triangles) and polymer **2** (closed squares) in acetonitrile. (b) Phosphorescence emission of complex **1** (open triangles) and polymer **2** (closed squares) in acetonitrile.

Table 1 Photophysical properties of iridium complex **1** and iridium polymer **2** at room temperature

	Emission[a] 298 K			
	λ/nm	φ_{sol}.[b]	φ_{film}[c]	τ/ns[d]
Iridium complex **1**	687	0.02	0.18	69
Iridium polymer **2**	687	0.01	0.09	47

[a] λ_{exc} = 350 nm. [b] De-aerated CH_3CN solution (10^{-4} M). [c] 5 wt% in PMMA. [d] Luminance emission lifetime in de-aerated CH_3CN solution (10^{-5} M), ± 10%.

absorption band at lower energies (~377 nm) is attributed to typical spin-allowed metal-to-ligand charge-transfer transitions (^{1}MLCT $d\pi(Ir) \rightarrow \pi^*$).[13,27,28]

The room-temperature emission spectra recorded in dilute, de-aerated acetonitrile solution upon excitation at 350 nm are also shown in Fig. 1. All the photophysical data are summarized in Table 1. The emission spectra exhibit a broad structureless band with a maximum at 687 nm for both complex **1** and polymer **2**. The CIE coordinates of both emission spectra are $x = 0.665$; $y = 0.334$, which correspond to a deep-red colour.[29] The broad emission band can be assigned, in a first approach, to a strong mixing between metal-to-ligand charge transfer (^{3}MLCT) and $^3\pi$–π^* transitions. This mixed character is typical of complexes containing a combination of orthometallating and neutral diimine ligands.[13,30–32] Identical emission spectra were obtained for the aerated solutions. The strong red shift observed for the emission of complex **1** (687 nm), when compared to that of the parent complex $[Ir(ppy)_2bpy][PF_6]$ (580 nm), is attributed to the stabilization of the LUMO. The introduction of the electron withdrawing ester groups in the bipyridine moiety, where the LUMO primarily resides, stabilizes this orbital and reduces the optical band gap.[30–33] The shape and position of the absorption and emission bands is practically the same for both complex **1** and polymer **2** indicating that the polymer backbone does not influence the energy of the electronic states involved in the absorption and emission processes.

As listed in Table 1, the photoluminescence quantum yields (φ) in de-aerated acetonitrile solution are low for both complex **1** (0.02) and polymer **2** (0.01). The low φ values are similar to those reported for other iTMCs emitting in the deep-red region of the visible spectrum,[15–18] and are corroborated by excited-state lifetimes of a few tens of nanoseconds (see Table 1).[34] In a recent work, Rothe *et al.* demonstrated that PLQE values measured in solution are not adequate to estimate the efficiency of the iTMC in LEC devices, and that this efficiency should be evaluated from PLQE measurements in thin films.[24] Measurements carried out on thin film of **1** and **2** diluted in polymethylmethacrylate (PMMA) yielded high φ values of 0.18 and 0.09, respectively. These PLQE values suggest that these compounds can be used as efficient luminescent materials for deep-red LECs. The PLQE recorded for the polymer is a half of that obtained for the free complex both in solution and in thin film. The polymer approach therefore seems to play a negative role in the photoluminescence properties of the complex.

Device characterization

Simple solid-state light-emitting devices were prepared using the iridium complex **1** and the iridium polymer **2** (LEC and PLEC, respectively). Prior to the deposition of the active layer, a thin layer (100 nm) of poly(ethylene dioxythiophene): polystyrene sulfonic acid (PEDOT:PSS) was spin-coated to increase the reproducibility of the devices. The active layer consisted primarily of either complex **1** or polymer **2**, which were spin-coated from an acetonitrile solution to yield a thickness of approximately 60–70 nm. In addition, small amounts of the ionic liquid (IL) 1-butyl-3-methylimidazolium hexafluorophosphate were added to decrease the turn-on time of the device. The molar ratio between the active iridium complex units and the IL molecules (Ir compound : IL) was 2 : 1. Previous to the deposition of aluminium as the cathode, the spin-coated films were heated on a hot plate at 80 °C during 5 h inside an inert atmosphere glove box. The aluminium electrode was thermally evaporated under vacuum ($<2 \times 10^{-6}$ mbar) to a thickness of 80 nm. Structured ITO-containing glass plates were used as the substrates. Device characterization was performed under inert atmosphere inside a glove box (< 0.1 ppm H_2O and < 0.1 ppm O_2).

Upon application of an external field of 3 V to the LEC and PLEC devices, a rapid increase in the current density and the luminance is observed (see Fig. 2A). The PLEC device exhibits a turn-on time—time needed to achieve maximum luminance—of 5.7 h that is much larger than that observed for the LEC device

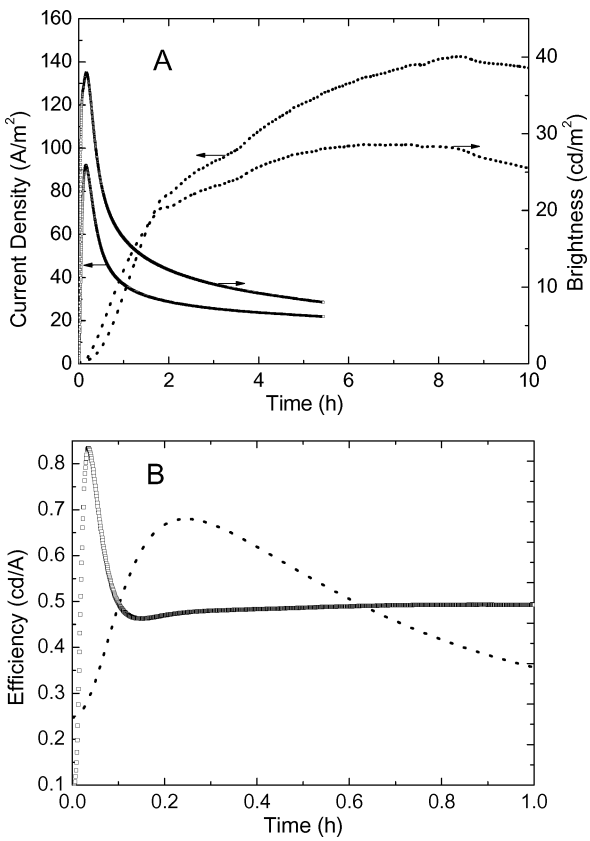

Fig. 2 A: Current density and luminance *vs.* time for the LEC device ITO/PEDOT:PSS/**1**:IL/Al (open squares) and the PLEC device ITO/PEDOT:PSS/**2**:IL/Al (dotted line). B: Efficiency *vs.* time at an applied voltage of 3 V for the LEC device ITO/PEDOT:PSS/**1**:IL/Al (open squares) and the PLEC device ITO/PEDOT:PSS/**2**:IL/Al (dotted line).

(0.17 h). The higher turn-on time indicates a lower mobility of the PF_6^- counter ions in the PLEC device.

Both devices show current density and luminance maximum values in the range of 90–140 A m^{-2} and 30–40 cd m^{-2}, respectively. These values result in similar current efficiencies of 0.83 and 0.68 cd A^{-1} and maximum power efficiencies of 0.87 and 0.71 lm W^{-1} for LEC and PLEC devices, respectively (see Fig. 2B).

As observed in Fig. 2A, the main difference between the LEC and the PLEC devices concerns the device stability. The PLEC device exhibit a lifetime—time required to reach the half of the maximum luminance ($t_{1/2}$)—of 37 h, which is almost two orders of magnitude longer than that recorded for the small-molecule based LEC device (0.52 h). The degradation mechanisms of LEC devices are not well understood but depend on the driving voltage, the film morphology and the complex used.[1,2] The only complex studied in detail in a LEC is $[Ru(bpy)_3]^{2+}$. Kalyuzhny *et al.* and Solzberg *et al.* concluded that the limited lifetime of $[Ru(bpy)_3]^{2+}$-based devices is most likely originated from a first-order degradation reaction involving the excited-state $[Ru(bpy)_3]^{2+}$* species and water molecules.[35,36] When a polymer-based $[Ru(bpy)_3]^{2+}$ compound was used, it was found that the stability was enhanced compared with the pure complex LEC device.[22] A similar effect is found here for the iridium complex **1** when it is attached to a polymer chain as in **2**. The increase in the lifetime originates from the spatial distribution of the complexes in the polymer that reduces the interaction between adjacent iTMCs and protects the complex against degradation reactions. Thus, although the photoluminescence efficiencies of the iridium polymer **2** are lower than those found for the iridium complex **1**, the incorporation of the polymer in a LEC device as the active component leads to better electroluminescent properties.

Fig. 3 shows the electroluminescence spectra recorded for the LEC and PLEC devices. The electroluminescence spectra show a shape similar to the photoluminescence spectra displayed in Fig. 1, indicating that the same optical transition is responsible for the light emission. The LEC device presents an emission maximum around 630 nm, whereas the PLEC device shows its maximum emission around 660 nm. The electroluminescence spectra therefore imply a blue shift of 57 nm (LEC device) and 27 nm (PLEC device) with respect to the photoluminescence spectra of the active compounds **1** and **2** in acetonitrile solution both emitting at 687 nm. The blue shift indicates that the excited state of the complex is destabilized in the device especially for **1**. The CIE coordinates[29] of the LEC and PLEC electroluminescence spectra are $x = 0.710$; $y = 0.283$ and $x = 0.691$; $y = 0.289$, respectively. These values are in the near-infrared range, an optical region where only few examples of emitting LEC devices have been reported.[15–18] The most striking one uses an osmium complex doped in a ruthenium-based active layer, for which slightly-higher efficiencies were obtained.[18] This is expected as in that case the emitter is isolated, but very poor morphological stability is foreseen for such a structure in contrast to the one presented in this work.

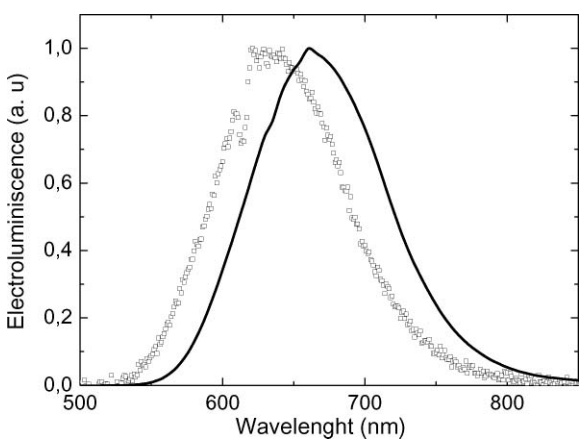

Fig. 3 Electroluminescence spectra for the LEC device ITO/PEDOT:PSS/**1**:IL/Al (open squares) and the PLEC device ITO/PEDOT:PSS/**2**:IL/Al (solid line) at an applied bias of 3 V.

Conclusions

A deep-red phosphorescent ionic iridium(III) complex has been synthesized and has been incorporated in a polymer. LEC devices using both the complex and the polymer as the electroluminescent active materials have been built up. The polymer version of the complex gives rise to devices with higher stabilities that emit light at longer wavelengths in the red (660 nm) than the devices using the small molecular weight complex (630 nm). The improved stability and the longer emission wavelength are attributed to a more uniform distribution of the active ionic transition-metal complexes imposed by the chemical linkage to the polymer backbone. This is one of the first examples of a polymeric iTMC-based optoelectronic device incorporating iridium(III) complexes that shows bright electroluminescence in a simple sandwiched architecture using air-stable electrodes. The synthetic strategy used can easily be adopted for the development of yellow-, green- and blue-light emitting cationic polymers by using slightly modified ligands in the iTMC. The work directed toward this goal is currently in progress.

Experimental

Materials and characterization methods

All reagents were purchased from commercial suppliers and used without further purification unless otherwise noted. 2,2′-bipyridine-4,4′-dicarboxylic acid,[37] 6-[(tetrahydro-2*H*-pyran-2-yl)oxy]-1-hexanol[38] and $[Ir(Tpy)_2Cl]_2$ (Tpy: Tolylpyridine)[39] were synthesized according to already published procedures. Commercial TLC plates (silica gel 60 F254, SDS) were used to monitor the progress of the reaction, with spots observed under UV light at 254 and 365 nm. Column chromatography was performed with silica gel 60A (particle size 40–63 μm, SDS).

NMR spectra were taken using either a 500 MHz Bruker Avance DRX 500, a 300 MHz Bruker Avance 300 or a Bruker AC-300. Gel permeation chromatography (GPC) analyses were carried out using an Agilent 1100 Series quaternary pump coupled to an Agilent 1100 series UV-vis detector with 5 mM NH_4PF_6 in DMF as the eluent on 10 μm particle size Phenogel 10u 50A and 10u 10∧3A (300 × 7.8 mm) columns at 70 °C and 1 mL min^{-1} flow. The GPC was calibrated using poly(styrene) standards. Ultraviolet-visible (UV-vis) absorption measurements were taken on a ThermoSpectronic Helios γ spectrophotometer. Differential scanning calorimetry (DSC) data were collected

using a PerkinElmer Instruments model Pyris 1 DSC with a ThermoHaake K20 refrigerator and a DC 30 controller. It was calibrated with indium and tin patrons. Infrared measurements were taken with a Fourier Transform (FT-IR) ThermoNicolet model IR 200 Spectrometer in attenuated total reflexion (ATR) with a germanium window. Mass spectra were obtained from a Bruker Reflex III matrix-assisted laser desorption/ionization time of flight (MALDI-TOF) spectrometer using dithranol as a matrix, or with a VG AutoSpec from Waters to record Positive-ion Fast Atom Bombardment (FAB^+) mass spectra using 3-nitrobenzyl alcohol (NBA) as the matrix solvent.

Synthesis

Diethyl-2,2′-bipyridine-4,4′-dicarboxilate (3). An alternative synthesis to the previously described[25] is used. A mixture of thionyl chloride (20 mL) and 2,2′-bipyridine-4,4′-dicarboxylic acid (2.32 g, 9.5 mmol) was refluxed 15 h under argon atmosphere. After all the solid was dissolved, the excess of $SOCl_2$ was distilled off and the residue redissolved in 60 mL of dry toluene. Then, a solution of absolute ethanol (1.1 mL, 874 mg, 19 mmol) and triethylamine (5.2 mL, 3.84 g, 38 mmol) in 10 mL of dry toluene was added. After heating for 4 h at 60 °C, the solvents were distilled off and the residue was chromatographed (silica gel, hexane–ethyl acetate = 3 : 1, $R_f = 0.41$) to afford 2.17 g (76%) of **3** as a white solid. δ_H(500 MHz; $CDCl_3$; Me_4Si) 1.45 (6 H, t, $J = 7.1$ Hz), 4.47 (4 H, q, $J = 7.1$ Hz), 7.91 (2 H, dd, $J = 4.9$ and 1.5 Hz), 8.87 (2 H, dd, $J = 4.9$ and 0.7 Hz), 8.95 (2 H, dd, $J = 1.5$ and 0.7 Hz).[26]

Iridium(III) complex (1). A solution of compound **3** (104.5 mg, 0.348 mmol) and $[Ir(Tpy)_2Cl]_2$ (157.1 mg, 0.139 mmol) in 15 mL of DCM was heated in the dark at 45 °C for 72 h. Elimination of the solvent and column chromatography (silica gel, DCM–MeOH = 93 : 7, $R_f = 0.25$) of the crude yielded 112.0 mg (47%) of a dark red solid. This solid (60 mg, 0.069 mmol) underwent anion exchange with NH_4PF_6 (337 mg, 2.07 mmol) in dry DMF (7 mL) at room temperature. The mixture was dissolved in DCM, and the organic phase was washed with water and dried over anhydrous Na_2SO_4. Elimination of the solvents at low pressure yielded a red solid (67 mg, quantitative). Mp (°C) 267–269. UV-vis ($CHCl_3$): λ_{max}/nm (log ε) 274, (4.61), 296 sh (4.53), 381 (3.97) and 525 (2.90). ν_{max}/cm^{-1} 1739, 1721, 1476, 1295, 1274, 1233, 878, 838, 773, 761 and 639. δ_H(300 MHz; $CDCl_3$; Me_4Si) 1.43 (6 H, t, $J = 7.1$ Hz), 2.13 (6 H, s), 4.49 (4 H, q, $J = 7.1$ Hz), 6.07 (2 H, d, $J = 1.0$ Hz), 6.86 (2 H, dd, $J = 7.9$ and 1.0 Hz), 7.03 (2 H, ddd, $J = 7.9$, 5.4 and 1.3 Hz), 7.50 (2 H, dd, $J = 5.4$ and 1.3 Hz), 7.58 (2 H, d, $J = 7.9$ Hz), 7.72 (2 H, td, $J = 7.9$ and 1.3 Hz), 7.84 (2 H, dd, $J = 7.9$ and 1.3 Hz), 8.00 (2 H, dd, $J = 5.6$ and 1.4 Hz), 8.11 (2 H, d, $J = 5.6$ Hz) and 8.99 (2 H, d, $J = 1.4$ Hz). δ_C(75 MHz; $CDCl_3$; Me_4Si) 14.12, 21.85, 62.96, 119.23, 123.27, 124.12, 124.20, 124.62, 127.93, 132.42, 138.23, 140.46, 140.66, 141.17, 148.78, 149.44, 151.33, 156.13, 163.02 and 167.29. MS MALDI-TOF m/z 829 ([M^+], calcd for $C_{40}H_{36}N_4O_4Ir$ 829).

Ethyl-6″-[(tetrahydro-2H-pyran-2‴-yl)oxy]hexyl-2,2′-bipyridine-4,4′-dicarboxylate (4). A mixture of 2,2′-bipyridine-4,4′-dicarboxylic acid (2.32 g, 9.5 mmol) and thionyl chloride (20 mL) was refluxed for 15 h under an argon atmosphere. Then, the excess of $SOCl_2$ was distilled off and the residue was dissolved in 60 mL of dry toluene and heated at 60 °C. Then, a solution of 6-[(tetrahydro-2*H*-pyran-2′-yl)oxy]-1-hexanol (1.93 g, 9.5 mmol), absolute ethanol (0.55 mL, 9.5 mmol) and dry Et_3N (5.2 mL, 38 mmol) in 20 mL of dry toluene was added dropwise. After 4 h, the solvent was evaporated and the residue chromatographed (silica gel, *n*-hexane–EtOAc = 3 : 1, $R_f = 0.39$) to give **4** (1.86 g, 42%) as a white solid. Mp (°C) 51–53. ν_{max}/cm^{-1} 2945, 1727, 1593, 1559, 1464, 1358, 1291, 1259, 1244, 1202, 1131, 1090, 1076, 1024, 980, 918, 864, 813, 762, 724, 695 and 667. δ_H(500 MHz; $CDCl_3$; Me_4Si) 1.45 (3 H, t, $J = 7.1$ Hz), 1.50 (8 H, m), 1.65 (2 H, m), 1.71 (1 H, m), 1.84 (3 H, m), 3.41 (1 H, m), 3.50 (1 H, m), 3.76 (1 H, m), 3.87 (1 H, m), 4.40 (2 H, t, $J = 6.7$ Hz), 4.47 (2 H, q, $J = 7.1$ Hz), 4.58 (1 H, m), 7.91 (2 H, m), 8.87 (2 H, d, $J = 4.9$ Hz) and 8.95 (2 H, s). δ_C(125 MHz; $CDCl_3$; Me_4Si) 14.19, 19.61, 25.40, 25.77, 25.90, 28.52, 29.55, 30.68, 61.79, 62.27, 65.86, 67.34, 98.80, 120.42, 120.46, 123.13, 138.85, 150.0, 156.41, 156.45, 165.04 and 165.09. MS MALDI-TOF m/z 457 ([M + H]$^+$, calcd for $C_{25}H_{32}N_2O_6$ 456).

From this chromatography, the diethyl ester **3** could also be separated ($R_f = 0.48$, 0.59 g, 21%). The other isolable by-product was the di(THPO-hexyl) ester ($R_f = 0.33$, 0.71 g, 13%). Mp (°C) 48–50. ν_{max}/cm^{-1} 2947, 1729, 1360, 1306, 1292, 1259, 1245, 1203, 1217, 1023, 1075, 763 and 696. δ_H(500 MHz; $CDCl_3$; Me_4Si) 1.44–1.74 (22 H, m), 1.84 (6 H, m), 3.41 (2 H, m), 3.50 (2 H, m), 3.76 (2 H, m), 3.86 (2 H, m), 4.40 (4 H, t, $J = 6.7$ Hz), 4.58 (2 H, t, $J = 3.5$ Hz), 7.91 (2 H, dd, $J = 4.9$ and 1.4 Hz), 8.87 (2 H, d, $J = 4.9$ Hz) and 8.95 (2 H, d, $J = 1.4$ Hz). δ_C(125 MHz; $CDCl_3$; Me_4Si) 19.62, 25.14, 25.79, 25.91, 28.53, 29.57, 30.70, 62.31, 65.92, 67.38, 98.83, 120.56, 123.19, 138.94, 150.00, 156.40 and 165.11. MS MALDI-TOF m/z 613 ([M + H]$^+$, calcd for $C_{34}H_{48}N_2O_8$ 612).

Ethyl-6″-hydroxyhexyl-2,2′-bipyridine-4,4′-dicarboxylate (5). A solution of HCl in EtOH (0.321 g of 35% HCl diluted with ethanol to a total volume of 3 mL) was added to a solution of **4** (913 mg, 2.0 mmol) in 15 mL of DCM. After 4 h at room temperature, the reaction mixture was extracted with 20 mL of DCM, washed with water and brine, and dried with anhydrous Na_2SO_4. Evaporation of the solvent and chromatographic purification (silica gel, *n*-hexane–EtOAc = 1 : 1, $R_f = 0.45$) yielded **5** (528 mg, 1.4 mmol, 71%) as a white solid. Mp (°C) 73–75. ν_{max}/cm^{-1} 3266, 2927, 2858, 1731, 1722, 1559, 1475, 1361, 1309, 1289, 1259, 1240, 1230, 1138, 1116, 1062, 1019, 993, 861, 763, 723, 696 and 668. δ_H(500 MHz; $CDCl_3$; Me_4Si) 1.45 (3 H, t, $J = 7.1$ Hz), 1.50 (4 H, m), 1.62 (2 H, m), 1.84 (2 H, m), 2.01 (1 H, br s), 3.68 (2 H, t, $J = 6.5$ Hz), 4.41 (2 H, t, $J = 6.7$ Hz), 4.47 (2 H, q, $J = 7.1$ Hz), 7.91 (2 H, m), 8.87 (2 H, m) and 8.94 (2 H, m). δ_C(125 MHz; $CDCl_3$; Me_4Si) 14.19, 25.33, 25.71, 28.43, 32.44, 61.85, 62.54, 65.83, 120.44, 120.53, 123.18, 123.19, 138.86, 138.92, 149.99, 150.02, 156.39, 156.40, 165.05 and 165.12. MS FAB^+ m/z 373 ([M + H]$^+$, calcd for $C_{20}H_{24}N_2O_5$ 372).

Ethyl-6″-methacryloxyhexyl-2,2′-bipyridine-4,4′-dicarboxylate (6). A solution of methacryloyl chloride (0.087 mL, 0.916 mmol) in 2 mL of dry THF was added dropwise under argon atmosphere to a solution of hydroxybipydirine 5 (84.4 mg, 0.227 mmol) in dry THF (8 mL) and dry Et_3N (0.120 mL, 0.916 mmol). The reaction mixture was stirred for 1 d at 50 °C to obtain a brown solution which was cooled to room temperature. After addition of AcOEt, the precipitated triethylamine hydrochloride was filtered off and the solution was washed successively with NaOH 10%, HCl 10% and water and dried with anhydrous Na_2SO_4. Column chromatography (silica gel, *n*-hexane–EtOAc = 5 : 1, $R_f = 0.29$)

gave 71.2 mg (71% yield) of a slightly yellowish viscous liquid. ν_{max}/cm^{-1} 2939, 2855, 1726, 1556, 1448, 1363, 1286, 1256, 1166, 1131, 1090, 1063, 1017, 764, 724, 693 and 659. δ_H(500 MHz; $CDCl_3$; Me_4Si) 1.45 (3 H, t, $J = 7.1$ Hz), 1.51 (4 H, m), 1.73 (2 H, m), 1.85 (2 H, m), 1.94 (3 H, s), 4.17 (2 H, t, $J = 6.6$ Hz), 4.41 (2 H, t, $J = 6.7$ Hz), 4.47 (2 H, q, $J = 7.1$ Hz), 5.54 (1 H, m), 6.10 (1 H, m), 7.91 (2 H, m), 8.87 (2 H, m) and 8.95 (2 H, m). δ_C(125 MHz; $CDCl_3$; Me_4Si) 14.21, 18.25, 26.61, 25.66, 28.47, 61.82, 64.48, 65.74, 120.46, 123.12, 123.17, 125.18, 136.38, 138.81, 138.89, 150.02, 156.40, 156.48, 165.05 and 165.10. MS FAB$^+$ m/z 441 ([M + H]$^+$, calcd for $C_{24}H_{28}N_2O_6$ 440).

Iridium(III) monomer (7). A solution of **6** (51.2 mg, 0.116 mmol) and $[Ir(Tpy)_2Cl]_2$ (52.7 mg, 0.047 mmol) in 5 mL of DCM was stirred in the dark at 45 °C for 12 h. After elimination of the solvent, chromatography of the residue (silica gel, DCM–MeOH = 93 : 7, $R_f = 0.42$) yielded a dark red solid in 48%. Mp (°C) 147–149. $\lambda_{max}(CHCl_3)/nm$ (log ε) 275 (4.61), 298 sh (4.54), 385 (3.93) and 530 (2.85). ν_{max}/cm^{-1} 2923, 2855, 1724, 1606, 1589, 1561, 1478, 1464, 1429, 1407, 1370, 1319, 1298, 1263, 1234, 1167, 1140, 1068, 1019, 932, 859, 819, 777, 763, 722, 702 and 639. δ_H(500 MHz; $CDCl_3$; Me_4Si) 1.42–1.50 (7 H, m), 1.71 (2 H, m), 1.83 (2 H, m), 1.92 (3 H, s), 2.13 (6 H, s), 4.14 (2 H, t, $J = 6.6$ Hz), 4.45 (2 H, m), 4.51 (2 H, q, $J = 7.1$ Hz), 5.54 (1 H, s), 6.06 (2 H, s), 6.08 (1 H, s), 6.87 (2 H, d, $J = 7.9$ Hz), 7.16 (2 H, dd, $J = 7.9$ and 5.0 Hz), 7.53 (2 H, d, $J = 5.0$ Hz), 7.60 (2 H, d, $J = 7.9$ Hz), 7.82 (2 H, t, $J = 7.9$ Hz), 7.88 (2 H, d, $J = 7.9$ Hz), 8.04 (1 H, d, $J = 5.6$ Hz), 8.05 (1 H, d, $J = 5.6$ Hz), 8.17 (1 H, d, $J = 5.6$ Hz), 8.18 (1 H, d, $J = 5.6$ Hz) and 9.07 (2 H, s). δ_C(125 MHz; $CDCl_3$; Me_4Si) 14.22, 18.33, 21.89, 25.43, 25.64, 28.48, 63.16, 64.44, 66.95, 119.54, 123.57, 124.10, 124.30, 124.85, 125.34, 128.00, 128.15, 132.37, 136.34, 138.73, 140.15, 140.28, 140.62, 141.32, 148.59, 149.10, 151.75, 156.00, 156.13, 162.83, 162.95, 167.31 and 167.51. MS MALDI-TOF m/z 969 ([M$^+$], calcd for $C_{48}H_{48}N_4O_6Ir$ 969).

Iridium(III) polymer (2). A solution of iridium complex **7** (140 mg, 0.140 mmol) and 2.8 mg of AIBN in 0.140 mL of dry DMF was heated at 60 °C under argon atmosphere for 23 h in a glass tube. Then, a DMF saturated solution of ammonium hexafluorophosphate was added maintaining the temperature for 1 h. The mixture was cooled to room temperature obtaining a red solid that was solved in CH_2Cl_2 and precipitated with cold MeOH three times. After drying at high vacuum, **2** was obtained (66 mg, 43% yield) as a red powder. $\lambda_{max}(CHCl_3)/nm$ (log ε) 273 (4.56), 294 sh (4.49), 382 (3.98), 526 (3.10). ν_{max}/cm^{-1} 2940, 1728, 1605, 1590, 1558, 1478, 1458, 1427, 1408, 1318, 1254, 1230, 1165, 1141, 1068, 840, 767 and 731. δ_H(500 MHz; CD_2Cl_2; Me_4Si) 0.80–2.20 (22 H), 3.80–4.50 (6 H), 6.05–6.15 (2 H), 6.75–7.05 (4 H), 7.35–8.25 (12 H) and 8.95–9.05 (2 H). δ_C(125 MHz; $CDCl_3$; Me_4Si) 13.94, 21.59, 25.52, 25.74, 28.39, 44.90, 62.95, 64.94, 66.80, 119.65, 123.21, 124.10, 124.17, 124.88, 124.96, 127.87, 127.97, 132.32, 138.43, 140.41, 140.99, 141.20, 148.64, 149.45, 151.74, 156.17, 156.23, 163.09, 163.20 and 167.29. GPC $\tilde{M}_n = 38\,000$, $\tilde{M}_w = 53\,000$, PDI = 1.4; DSC T_g (°C) 174.

Photophysical characterization

UV-vis absorption spectra were recorded using a Hewlett-Packard 8453 spectrophotometer. Room-temperature photo-excited fluorescent spectra were measured using a Varian-Carry Eclipse spectrofluorimeter. Quantum efficiencies were determined using the optically diluted method. Solutions of tris(2-phenylpyridine)iridium(III) in degassed acetonitrile and tris(bipyridine)ruthenium(II) in an aerated aqueous solution were used as references (0.40% and 0.028%, respectively).[27,40] The thin film quantum yield measurements were performed in air, using the quantum yield measurement system from Hamamatsu model C9920-01, using thin layers of the materials spin-coated on quartz substrates. The system is made up of an excitation light source, consisting of a xenon lamp linked to a monochromator, an integration sphere and a multi-channel spectrometer.

The excited state lifetimes were measured from fresh acetonitrile solutions, which were degassed by Ar bubbling for 30 min. They were deduced from time-resolved absorption spectroscopy utilising a laser flash-photolysis system based on a pulsed Nd:YAG laser, using 355 nm as exciting wavelength. The single pulses were approximately 10 ns duration and the energy was approximately 15 mJ per pulse. A Lo255 Oriel xenon lamp was employed as the detecting light source. The laser flash-photolysis apparatus consisted of the pulsed laser, the Xe lamp, a 77200 Oriel monochromator, and an Oriel photomultiplier (PMT) system made up of 77348 PMT power supply. The oscilloscope was a TDS-640A Tektronix. The output signal from the oscilloscope was transferred to a personal computer.

Device preparation and characterization

PEDOT:PSS was purchased from HC-Starck and solvents used were obtained from Aldrich. Indium tin oxide (ITO)-coated glass plates (15 Ω per square) were patterned using conventional photolithography (obtained from Naranjosubstrates, www.naranjosubstrates.com). The substrates were extensively cleaned using sonification in subsequently water-soap, water, and 2-propanol baths. After drying, the substrates were placed in a UV-ozone cleaner (Jelight 42-220) for 20 min.

The electroluminescent devices were prepared as follows. Transparent thin films of the active layer containing a polymer and the ionic liquid 1-butyl-3-methylimidazolium hexafluorophosphate molecules with molar ratio 2 : 1 were prepared. The active layer was obtained by spinning from acetonitrile solutions using concentrations of 20 mg mL^{-1} at 1000 rpm for 20 s, resulting in a 90 nm thick film. Prior to the deposition of the emitting layer, a 100 nm layer of PEDOT:PSS was deposited to increase the device preparation yield. The thickness of the films was determined using an Ambios XP1 profilometer. After spinning the organic layers, the samples were transferred to an inert atmosphere glovebox (< 0.1 ppm O_2 and H_2O, MBraun) and dried on a hot plate at 80 °C for 1 h. Aluminium metal electrodes (80 nm) were thermally evaporated using a shadow mask under vacuum ($< 1 \times 10^{-6}$ mbar) using an Edwards Auto500 evaporator integrated into an inert atmosphere glove box.

Current density and luminance *vs.* voltage were measured using a Keithley 2400 source meter and a photodiode coupled to a Keithley 6485 pico-ampmeter using a Minolta LS100 to calibrate the photocurrent. An Avantes luminance spectrometer was used to measure the EL spectrum. Lifetime data were obtained by applying a constant voltage over the device and monitoring the current flow and simultaneously the current generated by a Si-photodiode calibrated using a Minolta LS100 luminance meter.

Acknowledgements

This work has been supported by the European Union (Heteromolmat, STRP 516982), ESF Eurocores-05SONS-FP-021, and the Generalitat Valenciana, European FEDER funds and the Spanish Ministry of Science and Innovation-MICINN (grants MAT2006-28185-E, MAT2007-61584, CTQ2006-14987-C02-02, CTQ2007-67888/BQU, CTQ2008-05901/BQU, CONSOLIDER-INGENIO CSD2007-00007 and CSD2007-00010, ACOMP/2009/039, ACOMP/2009/056 and ACOMP/2009/269). J. L. R. R. acknowledges funding from CONSOLIDER-INGENIO program, and R. D. C. acknowledges the support of a FPU grant of the MICINN.

References

1 J. Slinker, D. Bernards, P. L. Houston, H. D. Abruña, S. Bernhard and G. G. Malliaras, *Chem. Commun.*, 2003, 2392–2399.
2 J. D. Slinker, J. Rivnay, J. S. Moskowitz, J. B. Parker, S. Bernhard, H. D. Abruña and G. G. Malliaras, *J. Mater. Chem.*, 2007, **17**, 2976–2989.
3 Q. Pei, G. Yu, C. Zhang, Y. Yang and A. J. Heeger, *Science*, 1995, **269**, 1086–1088.
4 C. H. Lyons, E. D. Abbas, J. K. Lee and M. F. Rubner, *J. Am. Chem. Soc.*, 1998, **120**, 12100–12107.
5 F. G. Gao and A. J. Bard, *J. Am. Chem. Soc.*, 2000, **122**, 7426–7427.
6 J. C. deMello, N. Tessler, S. C. Graham and R. H. Friend, *Phys. Rev. B: Condens. Matter Mater. Phys.*, 1998, **57**, 12951–12963.
7 J. D. Slinker, J. A. DeFranco, M. J. Jaquith, W. R. Silveira, Y. Zhong, J. M. Moran-Mirabal, H. G. Graighead, H. D. Abruña, J. A. Marohn and G. G. Malliaras, *Nat. Mater.*, 2007, **6**, 894–899.
8 E. A. Plummer, A. van Dijken, J. W. Hofstraat, L. De Cola and K. Brunner, *Adv. Funct. Mater.*, 2005, **15**, 281–289.
9 H. J. Bolink, E. Coronado, R. D. Costa, E. Ortí, M. Sessolo, S. Graber, K. Doyle, M. Neuburger, C. E. Housecroft and E. C. Constable, *Adv. Mater.*, 2008, **20**, 3910–3913.
10 S. Graber, K. Doyle, M. Neuburger, C. E. Housecroft, E. C. Constable, R. D. Costa, E. Ortí, D. Repetto and H. J. Bolink, *J. Am. Chem. Soc.*, 2008, **130**, 14944–14945.
11 R. D. Costa, E. Ortí, H. J. Bolink, S. Graber, C. E. Housecroft, M. Neuburger, S. Schaffner and E. C. Constable, *Chem. Commun.*, 2009, 2029–2031.
12 H. C. Su, H. F. Chen, F. C. Fang, C. C. Liu, C. C. Wu, K. T. Wong, Y. H. Liu and S. M. Peng, *J. Am. Chem. Soc.*, 2008, **130**, 3413–3419.
13 A. B. Tamayo, S. Garon, T. Sajoto, P. I. Djurovich, I. M. Tsyba, R. Bau and M. E. Thompson, *Inorg. Chem.*, 2005, **44**, 8723–8732.
14 H. C. Su, C. C. Wu, F. C. Fang and K. T. Wong, *Appl. Phys. Lett.*, 2006, **89**, 261118.
15 H. J. Bolink, L. Cappelli, E. Coronado and P. Gaviña, *Inorg. Chem.*, 2005, **44**, 5966–5968.
16 H. J. Bolink, E. Coronado, R. D. Costa, E. Ortí, P. Gaviña and S. Tatay, *Inorg. Chem.*, 2009, **48**, 3907–3909.
17 R. D. Costa, F. J. Céspedes-Guirao, E. Ortí, H. J. Bolink, J. Gierschner, F. Fernández-Lázaro and A. Sastre-Santos, *Chem. Commun.*, 2009, 3886–3888.
18 A. R. Hosseini, C. Y. Koh, J. D. Slinker, S. Flores-Torres, H. D. Abruña and G. G. Malliaras, *Chem. Mater.*, 2005, **17**, 6114–6116.
19 E. L. Williams, J. Li and G. E. Jabbour, *Appl. Phys. Lett.*, 2006, **89**, 083506.
20 C. Borek, K. Hanson, P. I. Djurovich, M. E. Thompson, K. Aznavour, R. Bau, Y. Sun, S. R. Forrest, J. Brooks, L. Michalski and J. Brown, *Angew. Chem., Int. Ed.*, 2007, **46**, 1109–1112.
21 D. R. Blasini, J. Rivnay, D.-M. Smilgies, J. D. Slinker, S. Flores-Torres, H. D. Abruña and G. G. Malliaras, *J. Mater. Chem.*, 2007, **17**, 1458–1461.
22 A. Wu, D. Yoo, J. K. Lee and M. F. Rubner, *J. Am. Chem. Soc.*, 1999, **121**, 4883–4891.
23 H.-C. Su, F. C. Fang, T. Y. Hwu, H. H. Hsieh, H. F. Chen, G. H. Lee, S. M. Peng, K. T. Wong and C. C. Wu, *Adv. Funct. Mater.*, 2007, **17**, 1019–1027.
24 C. Rothe, C.-J. Chiang, V. Jankus, K. Abdullah, X. Zeng, R. Jitchati, A. S. Batsanov, M. R. Bryce and A. P. Monkman, *Adv. Funct. Mater.*, 2009, **19**, 2038–2044.
25 G. Maerker and F. H. Case, *J. Am. Chem. Soc.*, 1958, **80**, 2745–2748.
26 P. G. Hoertz, A. Staniszewski, A. Marton, G. T. Higgins, C. D. Incarvito, A. L. Rheingold and G. J. Meyer, *J. Am. Chem. Soc.*, 2006, **128**, 8234–8245.
27 K. Nakamaru, *Bull. Chem. Soc. Jpn.*, 1982, **55**, 2697–2705.
28 H. J. Bolink, L. Cappelli, S. Cheylan, E. Coronado, R. D. Costa, N. Lardies, M. K. Nazeeruddin and E. Orti, *J. Mater. Chem.*, 2007, **17**, 5032–5041.
29 CIE, 1933.
30 J. Li, P. I. Djurovich, B. D. Alleyne, M. Yousufuddin, N. N. Ho, J. C. Thomas, J. C. Peters, R. Bau and M. E. Thompson, *Inorg. Chem.*, 2005, **44**, 1713–1727.
31 M. G. Colombo and H. U. Güdel, *Inorg. Chem.*, 1993, **32**, 3081–3087.
32 M. G. Colombo, A. Hauser and H. U. Güdel, *Inorg. Chem.*, 1993, **32**, 3088–3092.
33 F. Neve, M. LaDeda, A. Crispini, A. Bellusci, F. Puntoriero and S. Campagna, *Organometallics*, 2004, **23**, 5856–5863.
34 A. L. Medina-Castillo, J. F. Fernandez-Sanchez, C. Klein, M. K. Nazeeruddin, A. Segura-Carretero, A. Fernandez-Gutierrez, M. Graetzel and U. E. Spichiger-Keller, *Analyst*, 2007, **132**, 929–936.
35 G. Kalyuzhny, M. Buda, J. McNeill, P. Barbara and A. J. Bard, *J. Am. Chem. Soc.*, 2003, **125**, 6272–6283.
36 L. J. Soltzberg, J. D. Slinker, S. Flores-Torres, D. A. Bernards, G. G. Malliaras, H. D. Abruña, J. S. Kim, R. H. Friend, M. D. Kaplan and V. Goldberg, *J. Am. Chem. Soc.*, 2006, **128**, 7761–7764.
37 N. Garelli and P. Vierling, *J. Org. Chem.*, 1992, **57**, 3046–3051.
38 S. Nanda and J. S. Yadav, *Tetrahedron: Asymmetry*, 2003, **14**, 1799–1806.
39 H. Zhen, C. Jiang, W. Yang, J. Jiang, F. Huang and Y. Cao, *Chem.–Eur. J.*, 2005, **11**, 5007–5016.
40 A. Juris and L. Prodi, *New J. Chem.*, 2001, **25**, 1132–1135.